Jurnal Teknologi

Full Paper

ALUMINIUM - MODIFIED ZNO NANOPARTICLES SYNTHESIZED THROUGH CO-PRECIPITATION

Naif H. Al-Hardan[a]*, Muhammed Azmi Abdul Hamid[a], Mohd Firdaus-Raih[a], Lim Kar Keng[b]

[a]Department of Applied Physics, Faculty of Science and Technology, Universiti Kebangsaan Malaysia, 43600 UKM, Bangi Selangor, Malaysia
[b]Pusat Pengajian Citra Universiti, Universiti Kebangsaan Malaysia, 43600 Bangi, Selangor, Malaysia

Article history
Received
16 November 2021
Received in revised form
15 June 2022
Accepted
25 July 2022
Published Online
31 October 2022

*Corresponding author
naifalhardan@ukm.edu.my

Graphical abstract

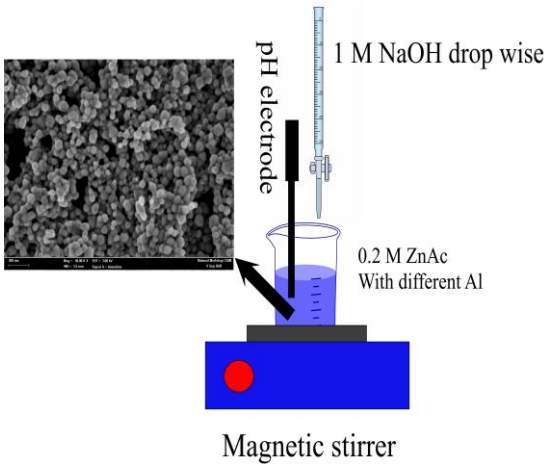

Abstract

The co-precipitation method is commonly used to produce nanoscale particles. The method was used to produce undoped and aluminium (Al) doped Zinc Oxide (ZnO) nanoparticles with doping percentages of 0 at%, 1 at%, 3 at%, and 5 at%. The samples were thermally treated in an atmospheric environment at 600 °C. The samples are then subjected to a number of characterization processes in order to investigate the effect of Al doping on the crystal structures, morphology, and chemical composition of the particle's surfaces. The doping process results in a polycrystalline structure of the Al doped ZnO with a predominant peak in the (101) phase. Furthermore, as doping content increased, the peak intensities of the (101) phase decreased. The results of the morphology through the field effect electron microscopy (FESEM) reveals the Al doping have a significant impact on the prepared samples.

Keywords: Doping process, Nanoparticles, Precipitation Method, ZnO nanostructures

Abstrak

Kaedah kepemendakan biasanya digunakan untuk menghasilkan zarah berskala nano. Kaedah ini digunakan untuk menghasilkan nanozarah Zinc Oxide (ZnO) yang tidak didop dan didop dengan aluminium (Al) dengan peratusan pengedopan pada 0 at%, 1 at%, 3 at% dan 5 at%. Sampel telah dirawat secara terma dalam persekitaran atmosfera pada 600°C. Sampel kemudiannya tertakluk kepada beberapa proses pencirian untuk mengkaji kesan pengedopan Al terhadap struktur hablur, morfologi, dan komposisi kimia permukaan zarah. Proses pengedopan menghasilkan struktur polihabluran ZnO terdop Al dengan puncak utama pada fasa (101). Tambahan pula, apabila kandungan pengedopan meningkat, keamatan puncak fasa (101) menurun. Keputusan morfologi melalui mikroskop electron kesan medan (FESEM) mendedahkan pengedopan Al mempunyai kesan yang ketara ke atas sampel yang disediakan.

Kata kunci: Proses pengedopan, nanozarah, kaedah mendakan, ZnO

© 2022 Penerbit UTM Press. All rights reserved

1.0 INTRODUCTION

The doping process plays a major role in the enhancement of the electrical and optical properties of functional materials [1-5]. Such as in gas sensors and biosensors [1, 2]. Zinc oxide (ZnO) is one of the most semiconductor compounds that has been under the focus of several research groups. The compound has a wide band gap (3.37 eV) with a high exciton energy of (60 meV) [6], which makes it one of the best candidates in the field of UV optoelectronics applications. Among these applications are UV sensors [3, 6, 7], UV light-emitting diodes [4] and UV laser diodes [8]. Furthermore, it is considered a safe biocompatible material. Due to the wide application of ZnO based devices, several methods have been deployed to synthesize it, such as the sol-gel method [9], hydrothermal method [10], chemical bath deposition [11], precipitation method [5], sputtering process [12] and others. These processes produce interesting structures where most are in the nano scale dimensions. Nanostructures are being a subject of attention because of their high surface-to-volume ratio. This will improve the sensing properties of sensors [13-15]. These manufacturing methods produce ZnO in different shapes, such as quantum dots (zero dimensional structures) [15], nanorods [10], nanowires [11] (one-dimensional structures) and others. Undoped ZnO exhibites n type conductivity, due to its native defects such as oxygen vacancies. Furthemore, udoped ZnO show a thermally unstable electrical properties and high resistivity [16]. To overcome this issue, ZnO is doped with differnt metels. Doping ZnO with group III ions (B^{3+}, Al^{3+}, Ga^{3+}, and In^{3+}), will overcome this issue. ZnO doped with aluminium (Al) is gaining popularity due to its nontoxicity, small ionic radius and low material cost with similar performance to several compound that been used in advanced technology applications such as transparent conductive oxide [16-18]. Mahmood *et al*., (2022) studied the effect of Al contents of co-precipitation prepared ZnO doped with Al (Al = 0, 2.5, 5, 7.5 and 10 wt%). The diffraction peaks of the XRD were significant enhanced with the Al contents [19]. Al doped ZnO was prepared via spray pyrolysis by Dhamodharan *et al*., (2017) at Al doping concentration (0–2.5 at.%) [20]. The prepared thin films were deployed for photoanode in solar cell applications. Sol–gel spin coating deposition process was used to prepare indium doped ZnO for opto-electronic applications [17]. The prepared films with different indium contents reveal high transmittance in the visible range, which make them potential for optoelectronic devices. ZnO nanowire was doped by europium (Eu) through electrodeposition process [21]. The prepared ZnO doped by Eu was applied for light emitting diodes. This group's findings show that Eu doped ZnO nanowires are a promising candidate for multispectral LEDs.

Due to the importance of the nano-scale structures of metal oxide semiconductors in different cutting-edge applications, we aimed in this report to study the effect of different Al contents on the phase structures and the morphology of the prepared undoped and Al-doped ZnO nanoparticles. The doping of Al was selected in the range of 1 at%, 3 at% and 5 at%. The low Al content in this study was chosen because of the low Al solubility in ZnO, as the goal was to maintain the phase structures of the prepared nanoparticles. The cost-effective co-precipitation method was employed to prepare the samples. The samples of ZnO produced with different doping contents undergo several characterization processes to study the effect of the doping process.

2.0 METHODOLOGY

Aluminium-doped zinc oxide (AZO) nanoparticles were prepared by the co-precipitation method. Zinc acetate dihydrate ($Zn(CH_3COO)_2$. $2H_2O$ > 99.5%) (Merck KGaA, Germany) and aluminium chloride ($AlCl_3 \cdot 6H_2O$ > 99.0%) (ChemPur) were used as precursors. Initially, 0.2 M of $Zn(CH_3COO)_2$. $2H_2O$ aqua solution was prepared by dissolving 4.39 g in 100 ml of deionized (DI) water (18 MΩ resistivity) under vigorous stirring at room temperature for 60 min. until a clear solution was obtained. $AlCl_3 \cdot 6H_2O$ was added to the solution considering the aluminium percentage in atomic ratio (Al/Zn) 0,1, 3, and 5 at%. Then, 1.0 M prepared sodium hydroxide solution (NaOH from Merck KGaA, Germany) was added to the above solution dropwise. The mixture turned white after a few drops. At this stage, the formation of zinc hydroxide sol takes place. The dropping process was stopped once the pH of the uniform white suspension reached 10. The stirrer process continued for another 1 h at room temperature.

The obtained powder was washed several times with distilled water and ethanol to remove impurities. The paste was collected by vacuum filtration of the undoped and doped ZnO aqueous solution through a membrane filter (0.45 µm in pore size), then the collected paste was dried at 100 °C for 24 h in a conventional oven. The dried powder was further calcined at 600 °C in Lindberg/Blue M™ box furnaces (Thermo Scientific™ USA) for 5 h at heating rate of 12 °C/min in an ambient atmosphere. The prepared powders were characterized for their phase structures and morphology using XRD and FESEM.

3.0 RESULTS AND DISCUSSION

3.1 The Phase Structural Analysis

Initially, all the undoped ZnO and Al-doped ZnO samples prepared by the co-precipitation method were white in color and yellowish in color when doped with 5 at% Al. Figure 1 depicts the XRD pattern of the prepared powders with the scanning Bragg angle of 20° to 80°. The figure reveals the polycrystalline structure of the powders produced

with high-quality crystallinity, as indicated by the sharp XRD peaks. The polycrystalline nature of the prepared powders shows the same structure quality even after doping with 1 to 5 at% Al. The peaks appeared in the pattern match well with the ZnO hexagonal structure wurtzite structure according to (JCPDS No. 36-1451). However, the pattern shows a weak peak of Al_2O_3 at concentration 3 and 5 at% at Bragg angle 45.44° which belongs to the γ-alumina phase of Al_2O_3. This might be due to the low Al solubility in ZnO at this range of doping [22, 23].

The appeared diffraction patterns are indexed to (100), (002), (101), (102), (110), (103), (200), (112) (004) and (202) phases of the ZnO structure. It is worth mentioning that there was an enhancement in the peak's intensity of the (101) phase after doping with Al. This implies the success of the doping process of Al in the host ZnO structure. However, the intensity of the peak starts to decrease after doping reaches 3 at% and 5 at%, probably due to the destruction and reorganization of the ZnO structure [9]. It was reported that the thermodynamic limit of solubility of Al in ZnO is in the rang 2–3 at% range [16, 23]. However, it the current case, the clear diffraction peaks that belong to the ZnO structure prove that the limit of solubility might be higher than that was reported before. Lu *et al.*, (2006) reported higher solubility of Al in ZnO in the 20–30 at % range [23]. The degradation of crystallinity could be attributed to the deformation of the lattice structure due to the difference in the ionic radii of Al^{3+} (~0.053 nm) and Zn^{2+} (~0.075 nm) [9, 18].

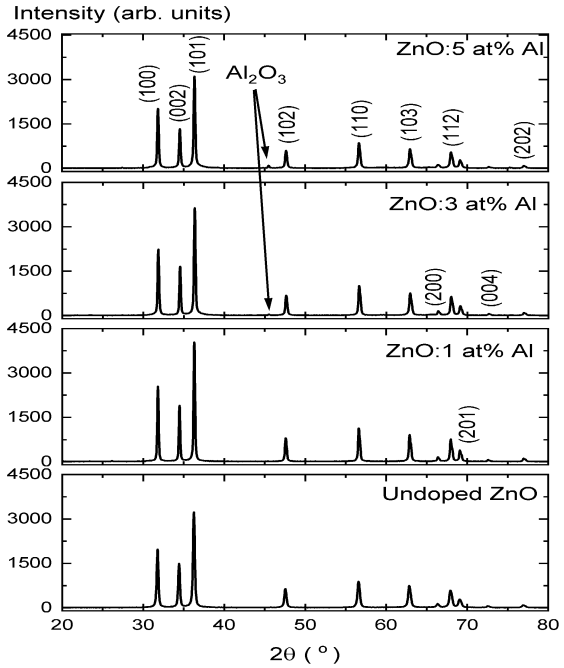

Figure 1 The XRD pattren of the prepared undoped ZnO and doped with 1 at%, 3 at% and 5 at% Al

From the data obtained from the XRD analysis, the lattice spacing for the prepared undoped and doped ZnO structures with different Al content can be estimated using the formula below [24].

$$2d_{hkl}\sin\theta = n\lambda \quad (1)$$

Whereby the lattice constants of the ZnO wurtzite structure were calculated according to [24]

$$\frac{1}{d_{hkl}^2} = \frac{4}{3}\left(\frac{h^2+hk^2+k^2}{a^2}\right)+\frac{l^2}{c^2} \quad (2)$$

The lattice parameters of the wurtzite structure a and c were calculated using the following expressions [2]

$$a = \left(\frac{\lambda}{\sqrt{3}\sin\theta_{(100)}}\right) \quad and \quad c = \frac{\lambda}{\sin\theta_{(002)}} \quad (3)$$

Furthermore, the average crystallite size (D_{ave}) of the prepared samples is evaluated using the Debye–Scherrer formula [24]. From the reciprocal, the dislocation density δ could be found, which represents the amount of deficiency in the film [2]. In this case, we shall select the prominent diffraction peak of the (101) phase. The results are shown in Table 1, detailing the ratio of 2θ, D_{ave}, d_{101}, a, c, and c/a of the prepared undoped ZnO and doped with Al at contents of 0, 1, 3, and 5at%. Doping Al into the ZnO crystal will have a substantial influence on the ZnO crystal structures, based on the XRD data and the results derived using Equation (1)-(3). Initially, there is a shift in the peak position of the (1 0 1) plane toward the lower Bragg angle, which could be attributable to the smaller ionic radii of Al^{3+} compared to Zn^{2+} [9]. The crystallite size of the samples decreased from 87.41 to 8.31 nm with increasing Al content from 0 to 5 at%. This is attributed to the replacement of Zn^{2+} ions by Al^{3+} ions during formation of the Al doped ZnO powders.

Table 1 show the results estimated from Equation (1)-(3) for the crystal structure parameters with the Al contents in the undoped and doped ZnO with Al

Al/Zn	0.0%	1.0 at%	3.0 at%	5.0 at%
$2\theta_{(101)}$ (°)	36.40	36.30	36.34	36.34
D_{ave} (nm)	87.41	48.54	17.84	8.31
δ (nm^2)	$1.31x10^{-4}$	$4.24x10^{-4}$	$3.14x10^{-3}$	$1.45x10^{-2}$
d_{101}(nm)	0.247	0.247	0.247	0.247
a (nm)	0.285	0.285	0.285	0.285
c (nm)	0.493	0.494	0.494	0.494
c/a	1.732	1.732	1.732	1.732
FWHM (°)	0.242	0.199	0.210	0.213

As the Al ions are smaller than the Zn ions, they consequently reduce the crystallite size. The same trend was noticed by Sahay and Nath, (2008) [25]. Similarly, δ was incremented from $1.31x10^{-4}$ to $1.45x10^{-2}$ nm^{-2} implying that the defects have increased in line with the Al concentration. It was reported that an increase in doping concentration deteriorates the crystallinity of the ZnO crystal structure [26]. The lattice index for both (a) and (c) is close to the standard ZnO according to (JCPDS No. 36-1451) [27]. Furthermore, the ratio (c/a) demonstrates that the produced samples of undoped and doped ZnO are almost a perfect wurtzite structure [27]. The full-width at half-maximum (FWHM) of the X ray diffraction peak was reported to be sensitive to the variation in the grain distortion, dislocation density and residual stresses in the material [28]. In Table 1, the reported values of the FWHM in this study show a significant decreased in its value once the Al is introduced to the ZnO crystal. The values then show a trend of slight increase with the increase of the Al contents. The same trend was noticed by several groups [29, 30]. This manifest the decrease in the crystallite size as the Al contents are increased due to the difference in the ionic radii of Al^{3+} (~0.053 nm) and Zn^{2+} (~0.075 nm).

3.2 Morphology Characterization

The FESEM microimages were recorded at 50,000x magnification. Figure 2 (a, b, c, and d) reveals the micro images of the morphology of the synthesized undoped and Al (1, 3 and 5) at% doped ZnO samples, respectively.

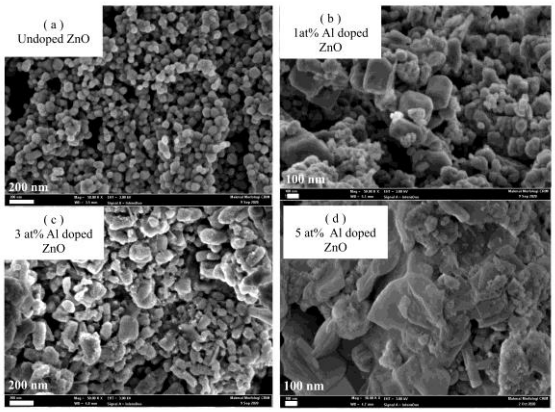

Figure 2 The FESEM microimages of the undoped and doped ZnO with (a) 0 at%, (b) 1 at%, (c) 3 at% and (d) 5 at% Al

The images highlighted the nano scale size with uniform distribution of the spherical particles with an average grain size of 60 ± 8 nm for the undoped ZnO. Interestingly, a hexagonal rod structure starts to grow at 1 at% Al doping with a clear and sharp surface edge, this might indicate a better crystallinity as observed by the XRD [21]. However, increasing the Al doping converts the structures into irregular shapes and multiple-sized grain structures and as the dopant is increased to 5 at% the grains start to fuse and randomly oriented large grains are formed. There is the possibility that defects induced larger grains to form instead of typical hexagonal structures, which was obvious at 5 at%. The defects (dislocation density) increased with the dopants can also be seen in the XRD results.

The elemental composition of the synthesised powders was analyzed by EDX on a selected area on the surface of the samples. The doped samples reveal the existence of Al in addition to the main components (Zn and O). This implies the successful doping of Al into the ZnO structure. Figure 3 presents the EDX results of the 3 at% Al.

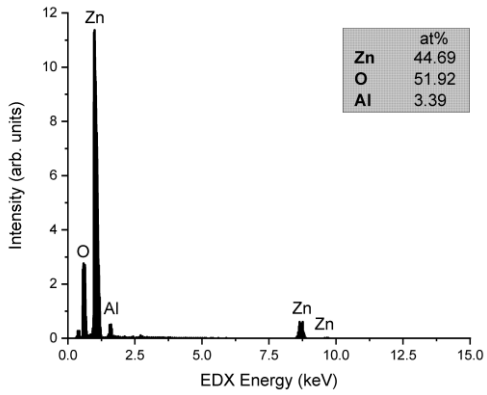

Figure 3 The EDX spectra of the 3 at% Al doped ZnO

4.0 CONCLUSION

A simple synthesis method is applied to form undoped and doped ZnO with Al content in the range of 1at%, 3at%, and 5at%. The synthesis samples reveal a polycrystalline structure with a predominant peak at the (101) phase. The peak intensities of the (101) phase decreased with the doping content (3 and 5 at%). The morphology of the synthesis samples was significantly affected by the Al dopants. The process proves to be an affordable path for growing high quality undoped and doped ZnO for different advanced applications.

Acknowledgement

This work was supported by the Universiti Kebangsaan Malaysia (UKM) through short-term grant number GGPM-2020-047 (UKM). The authors are also grateful to the Centre for Research and Instrumentation Management (CRIM) at UKM for providing the FESEM, EDX, and XRD measurements.

References

[1] Yoo, R., Li, D., and Rim, H. J. 2018. High Sensitivity in Al-Doped Zno Nanoparticles for Detection of Acetaldehyde. *Sensors and Actuators B: Chemical.* 883-888. DOI: https://doi.org/10.1016/j.snb.2018.03.102.

[2] Al-Khalqi, E. M., Abdul Hamid, M. A., and Al-Hardan, N. H. 2021. Highly Sensitive Magnesium-Doped ZnO Nanorod pH Sensors Based on Electrolyte–Insulator–Semiconductor (EIS) Sensors. *Sensors.* 21: 2110. DOI: https://doi.org/10.3390/s21062110.

[3] Mondal, S., Ghosh, S., and Basak, D. 2021 Extraordinarily High Ultraviolet Photodetection by Defect Tuned Phosphorus Doped ZnO Thin Film on Flexible Substrate. *Materials Research Bulletin.* 144: 111490. DOI: https://doi.org/10.1016/j.materresbull.2021.111490.

[4] Madhu, C., Kaur, I., and Kaur, N. 2018. Design and Synthesis of Imine Linked ZnO Nanoparticles Functionalized With Al(III), Candidate for Application in Light Emitting Diodes. *Journal of Materials Science: Materials in Electronics*. 29: 7785-7791. DOI: https://doi.org/10.1007/s10854-018-8776-y.

[5] Belkhaoui, C., Mzabi, N., and Smaoui, H. 2019. Investigations on Structural, Optical and Dielectric Properties of Mn Doped ZnO Nanoparticles Synthesized by Co-Precipitation Method. *Materials Research Bulletin.* 111: 70-79. DOI: https://doi.org/10.1016/j.materresbull.2018.11.006.

[6] Al-Hardan, N. H., Mohd Rashid, M. M., and Abdul Aziz, A. 2019. Low Power Consumption UV Sensor based on n-ZnO/p-Si Junctions. *Journal of Materials Science: Materials in Electronics.* 30: 19639-19646. DOI: https://doi.org/10.1007/s10854-019-02337-2.

[7] Al-Hardan, N. H., Abdul Hamid, M. A., and Ahmed, *N. M.* 2016. Ag/ZnO/p-Si/Ag Heterojunction and their Optoelectronic Characteristics under Different UV Wavelength Illumination. *Sensors and Actuators A: Physical.* 242: 50-57. DOI: https://doi.org/10.1016/j.sna.2016.02.036.

[8] Duman, C., and F. Kaburcuk, 2019. A Numerical Study of ZnO Random Lasers using FDTD Method. *Optik.* 181: 993-999. DOI: https://doi.org/10.1016/j.ijleo.2018.12.136.

[9] Islam, M. R., Rahman, M., and Farhad, *S. F. U.* 2019. Structural, Optical and Photocatalysis Properties of Sol–gel Deposited Al-doped ZnO Thin Films. *Surfaces and Interfaces* .16: 120-126. DOI: https://doi.org/10.1016/j.surfin.2019.05.007.

[10] Al-Hardan, N. H., Jalar, A., and Hamid, M. A. A. 2014 The Room-temperature Sensing Performance of ZnO Nanorods for 2-methoxyethanol Solvent, *Sensors and Actuators B: Chemical.* 203: 223-228. DOI: https://doi.org/10.1016/j.snb.2014.06.120.

[11] Villafuerte, J., Donatini, F., Kioseoglou, J. 2020. Zinc Vacancy–Hydrogen Complexes as Major Defects in ZnO Nanowires Grown by Chemical Bath Deposition. *The Journal of Physical Chemistry C.* 124: 16652-16662. DOI: https://doi.org/10.1021/acs.jpcc.0c04264.

[12] Misra, P., Ganeshan, V., and Agrawal, N. 2017. Low Temperature Deposition of Highly Transparent and Conducting Al-doped ZnO Films by RF Magnetron Sputtering. *Journal of Alloys and Compounds.* 725: 60-68. DOI: https://doi.org/10.1016/j.jallcom.2017.07.121.

[13] Tan, C., and Zhang, H. 2015. Wet-chemical Synthesis and Applications of Non-layer Structured Two-dimensional Nanomaterials. *Nature Communications.* 6: 7873. DOI : https://doi.org/10.1038/ncomms8873.

[14] Karim, S. S. A., Nadzirah, S., and Kazmi, J. 2021. Zinc Oxide Nanorods-based Immuno-field-effect Transistor for Human Serum Albumin Detection. *Journal of Materials Science.* 56: 15344-15353. DOI : https://doi.org/10.1007/s10853-021-06288-0.

[15] Zubair, M. Mustafa, M., and Ali, A. 2015. Improvement of Solution based Conjugate Polymer Organic Light Emitting Diode by ZnO–graphene Quantum Dots. *Journal of Materials Science: Materials in Electronics.* 26: 3344-3351. DOI: https://doi.org/10.1007/s10854-015-2837-2.

[16] Alkahlout, A., N. Al Dahoudi, N., and Grobelsek, I. 2014. Synthesis and Characterization of Aluminum Doped Zinc Oxide Nanostructures via Hydrothermal Route. *Journal of Materials.* 2014: 235638. DOI : https://doi.org/10.1155/2014/235638.

[17] Koralli, P., Fiat Varol, S., and Mousdis, G. 2022. Comparative Studies of Undoped/Al-Doped/In-Doped ZnO Transparent Conducting Oxide Thin Films in Optoelectronic Application. *Chemosensors.* 10: 162. DOI: https://doi.org/10.3390/chemosensors10050162.

[18] A. C. Badgujar, B. S. Yadav, G. K. Jha *et al.* 2022 Room Temperature Sputtered Aluminum-Doped ZnO Thin Film Transparent Electrode for Application in Solar Cells and for Low-Band-Gap Optoelectronic Devices. *ACS Omega.* 7: 14203-14210. DOI: https://doi.org/10.1021/acsomega.2c00830.

[19] Mahmood, A., Munir, T., and Fakhar-e-Alam. 2022. Analyses of Structural and Electrical Properties Of Aluminium Doped ZnO-NPs by experimental and Mathematical Approaches. *Journal of King Saud University - Science.* 34: 101796. DOI: https://doi.org/10.1016/j.jksus.2021.101796.

[20] Dhamodharan, P., Manoharan, C., and Bouo budina, M. 2017. Al-doped ZnO Thin Films Grown Onto ITO Substrates As Photoanode in Dye Sensitized Solar Cell. *Solar Energy.* 141: 127-144. DOI: https://doi.org/10.1016/j.solener.2016.11.029.

[21] Lupan, O., Pauporté, T., and Viana, *B.* 2013. Eu-doped ZnO Nanowire Arrays Grown by Electrodeposition. *Applied Surface Science.* 282: 782-788. DOI: https://doi.org/10.1016/j.apsusc.2013.06.053.

[22] Hou, Y., A. M. Soleimanpour,A. M., and Jayatissa, A. H. 2013. Low Resistive Aluminum Doped Nanocrystalline Zinc Oxide for Reducing Gas Sensor Application via Sol–gel Process. *Sensors and Actuators B: Chemical.* 177: 761-769. DOI: https://doi.org/10.1016/j.snb.2012.11.085.

[23] Lu, J. G., Ye, Z. Z., and Zeng, Y. J. 2006. Structural, Optical, and Electrical Properties of (Zn,Al)O Films Over a Wide Range of Compositions. *Journal of Applied Physics.* 100: 073714. DOI: https://doi.org/10.1063/1.2357638.

[24] V. Kumar, V., Kumar, V., and Som, S. 2014. Effect of Annealing on the Structural, Morphological and Photoluminescence Properties of ZnO Thin Films Prepared by Spin Coating. *Journal of Colloid and Interface Science.* 428: 8-15. DOI: https://doi.org/10.1016/j.jcis.2014.04.035.

[25] Sahay, P. P., and Nath, R. K. 2008. Al-Doped Zinc Oxide Thin Films for Liquid Petroleum Gas (LPG) Sensors. *Sensors and Actuators B: Chemical.* 133: 222-227. DOI: https://doi.org/10.1016/j.snb.2008.02.014.

[26] Li, L. J., Deng, H., and Dai, L. P. 2008. Properties of Al Heavy-Doped ZnO Thin Films by Rf Magnetron Sputtering. *Materials Research Bulletin.* 43: 1456-1462. DOI: https://doi.org/10.1016/j.materresbull.2007.06.042.

[27] Al-Hardan, N. H., Hamid, M. A. A., and Jalar, A. 2017. Synthesis of Magnesium-Doped ZnO Rods Via Hydrothermal Method: A Study of the Structural and Optical Properties. *ECS Journal of Solid State Science and Technology.* 6: 571-577. DOI: https://doi.org/10.1149/2.0021709jss.

[28] Vashista, M., and Paul, S. 2012. Correlation Between Full Width at Half Maximum (FWHM) of XRD Peak with Residual Stress on Ground Surfaces. *Philosophical Magazine.* 92: 4194-4204. DOI: https://doi.org/10.1080/14786435.2012.704429.

[29] Sabeeh, S. H., and Jassam, R. H. 2018. The Effect of Annealing Temperature and Al Dopant on Characterization of ZnO Thin Films Prepared by Sol-Gel Method. *Results in Physics.* 10: 212-216. DOI: https://doi.org/10.1016/j.rinp.2018.05.033.

[30] Ma, H. 2019. Effects of Aluminum Doping on the Structural and Optical Properties of ZnO Nanorods Grown on Highly

Conductive Films. *Journal of Materials Science: Materials in Electronics*. 30: 12532-12539. DOI: https://doi.org/10.1007/s10854-019-01613-5.